

The Unusual Near-Infrared Morphology of the Radio Loud Quasar 4C +09.17*

L. Armus¹, G. Neugebauer¹, M.D. Lehnert², K. Matthews¹

¹ Palomar Observatory, Caltech, Pasadena, CA 91125

² Sterrewacht Leiden, Postbus 9513, 2300RA Leiden The Netherlands

* Based on observations with the W.M. Keck Observatory, which is operated by the California
Institute of Technology and the University of California

Received _____; accepted _____

ABSTRACT

Near-infrared images of the luminous, high redshift ($z = 2.1108$) radio loud quasar 4C +09.17 reveal a complex structure. The quasar ($K = 15.76$ mag) is surrounded by three “companion” objects having $17.9 < K < 20.2$ mag at radii of $1.7'' < \Delta r < 2.9''$, as well as bright, diffuse emission. The brightest companion has a redshift of $z = 0.8384$ (Lehnert & Becker 1997) and its optical-infrared colors (Lehnert et al. 1997) are consistent with a late-type spiral galaxy at this redshift with a luminosity of about $2L^*$. This object is likely the galaxy responsible for the strongest MgII absorption line system seen in the spectrum of 4C +09.17 by Barthel et al. (1990). Redshifts are not available for the remaining two companions. The red colors of the second brightest companion appear most consistent with a high redshift star-forming galaxy at $z > 1.5$. If this object is at the redshift of 4C +09.17 it has a luminosity of about $7L^*$. The faintest companion has colors which are unlike those expected from either a spiral or an E/S0 galaxy at any redshift associated with the 4C +09.17 system. Since this object lies along the same direction as the radio jet/lobe of 4C +09.17, as well as the extended Ly α emission mapped by Heckman et al. (1991) we suggest that this component can be explained as a combination of strong line emission and scattered QSO light. The resolved, diffuse emission surrounding 4C +09.17 is bright, $K \sim 17.0$ mag, and about one magnitude redder in J-K than the quasar. If this emission is starlight, a very luminous elliptical host galaxy is implied for 4C +09.17. Scattered and reddened AGN light, emission line gas, and flux from absorbing galaxies along the line of sight may all contribute to this emission.

Subject headings: Quasars: General, Quasars: Individual - 4C +09.17, Galaxies: photometry - infrared

1. Introduction

At low redshifts, quasars often sit at the centers of luminous galaxies (Hutchings, Crampton & Campbell 1984, Smith et al. 1986, Bahcall et al. 1997). In general, radio loud quasars, those with monochromatic radio powers at centimeter wavelengths of more than $10^{25} - 10^{26}$ W Hz $^{-1}$ and radio-to-optical monochromatic luminosity ratios larger than ~ 100 - see Kellerman et al. (1988) and Schneider et al. (1992), inhabit elliptical galaxies, while radio quiet quasars tend to be found in spiral galaxies (Boroson & Oke 1984; Malkan 1984; Boroson, Persson & Oke 1985; Smith et al.). Furthermore, the host galaxies of radio loud quasars tend to be more luminous by about one magnitude in the visual than their radio quiet counterparts (Smith et al.). The reason for these apparent dichotomies are not well understood. Images of low redshift luminous ($M_B < -23$ mag) quasars obtained with the Hubble Space Telescope show a wide variety of host galaxy morphologies including both elliptical and spiral systems as well as highly disturbed galaxies which may be interacting with and/or accreting close companions (Bahcall et al., Disney et al. 1995, Hutchings & Morris 1995). In addition, recent deep infrared imaging (Neugebauer, Matthews & Armus 1995 ; Mcleod & Rieke 1995) has proven very effective in finding smooth host galaxies and faint companions around some low redshift quasars. That the nature of quasar host galaxies even at low redshift is still a matter of some debate is evidenced by the recent discussions concerning the Hubble Space Telescope results presented by Bahcall et al., and the efforts made to reconcile these results with ground based measurements made at longer wavelengths (e.g. McCleod & Rieke). In particular, the fact that 50% of the radio quiet quasars imaged by Bahcall et al. seem to have elliptical hosts has challenged the apparent clear-cut distinction between the hosts of radio quiet and radio loud quasars.

At redshifts above $z \sim 2$, dis-entangling host galaxy light from AGN light is made difficult by the relative faintness of the host galaxy as well as the blurring effects of atmospheric seeing. However, it is precisely at these redshifts that studies of the near environments of quasars offer the most hope of furnishing clues to the early evolution of AGN and galaxies. It is now well established that the redshift regime of $z \sim 2 - 3$ represents a real maximum in the number density

of luminous quasars (Hartwick & Schade 1990; Schmidt, Schneider & Gunn 1995). Between these redshifts and the present, the number density of luminous quasars has dropped by more than a factor of 1000, suggesting very strong cosmic evolution. If high redshift quasars sit at the centers of luminous host galaxies, the peak in the quasar density at $z \sim 2 - 3$ may signal an epoch where luminous galaxies were being hierarchically assembled (e.g. Carlberg & Couchman 1989).

As part of a K-band imaging survey of the Mpc-scale environments of a large sample of high redshift quasars with the W.M. Keck Telescope, we have imaged a very complex system around the $z = 2.1108$, radio loud quasar, 4C +09.17 at RA(1950)=04h45m37.12s, DEC(1950)= +09d45'37.2''. This object serves as an excellent example not only of the wealth of detail that a deep imaging program of this magnitude will provide, but also of the various pitfalls associated with inferring the properties of the host galaxies and companions of high redshift quasars.

4C +09.17 was previously found to have an extended, asymmetric Ly α nebula with a luminosity of about 1.6×10^{44} erg s $^{-1}$ by Heckman et al. (1991). Lehnert et al. (1992) imaged 4C +09.17 in the K-band and found resolved emission at radii from 1'' to 6'' with a $K \sim 17.5 \pm 0.4$ mag. This emission appeared asymmetric, but the true morphology of the nebulosity was unclear. The Keck J and K-band data presented here show a group of three objects within 3'' of the quasar as well as very bright diffuse near-infrared emission and they allow a determination of the magnitudes and colors for each of the components.

Barthel et al. (1990) quote a number of emission line redshifts for 4C +09.17 from the CIV, HeII and CIII] features, spanning a range of $z = 2.1085$ to $z = 2.1114$. We adopt the average emission line redshift of $z = 2.1108$, as determined by Barthel et al. as the systemic redshift of 4C +09.17. In addition to the emission lines, there are four absorption line systems in the spectrum of 4C +09.17 (Barthel et al.). Two of these are MgII systems at redshifts of $z = 0.839$ and $z = 1.466$, the former being significantly stronger than the latter, with rest frame equivalent widths (EQW) of 2.68\AA vs. 0.46\AA , respectively. In addition, there is a CIV absorption system at a redshift of $z = 2.107$, having a rest frame EQW of 2.3\AA . Finally, there is a CIV absorption line system with $z_{abs} \sim z_{em}$ and a rest frame EQW of 1.4\AA .

Throughout this paper we adopt $H_o = 75 \text{ km s}^{-1} \text{ Mpc}^{-1}$ and $q_o = 0$, so that the distance to 4C +09.17 is 5576 Mpc, and $1''$ on the sky is equivalent to 8.8 kpc in projection. In order to compare the observed infrared magnitudes to the expected rest frame values of typical galaxies in the local Universe, we employ the optical luminosity function of Mobasher, Sharples & Ellis (1993), such that a spiral galaxy has a characteristic absolute magnitude, $M_B^* = -20.49$ mag, while an E/S0 galaxy has a characteristic absolute magnitude, $M_B^* = -20.24$ mag, following Schechter (1976), and converting the Mobasher, Sharples & Ellis values into ones appropriate for an $H_o = 75 \text{ km s}^{-1} \text{ Mpc}^{-1}$. Combining these characteristic absolute magnitudes with the spectral energy distributions of Coleman, Wu & Weedman (1980), we estimate that the apparent K magnitudes of an L* spiral and E/S0 galaxy at a redshift of $z = 2.1108$ are K= 21.46 mag and K= 20.99 mag, respectively.

2. Observations and Data Reduction

Observations of 4C +09.17 were made at the W.M. Keck Observatory on the nights of 13 Feb 1995 and 5 Oct 1995 UT with the Near Infrared Camera (NIRC). The quasar was imaged through a broad-band K filter ($2.0\text{-}2.45\mu\text{m}$) during both runs, and through a broad-band J filter ($1.12\text{-}1.37\mu\text{m}$) during the Oct 1995 observing run. The plate scale of the 256x256 InSb array is $0.15''$ per pixel. The total integration time through the K filter was 1080 seconds in Feb 1995 and 540 seconds in Oct 1995. The total integration time through the J filter was 540 seconds in Oct 1995. In each case, individual images of 60 seconds duration have been taken with the quasar moved by $\sim 10''$ on the array between successive exposures. Sky and flat field frames were generated from the data by combining exposures in groups of 7 – 9 using either a clipped mean or median filtering technique. An offset guider employing a visual wavelength CCD was used to accurately maintain the telescope tracking. Since the quasar is visible in each 60 second exposure, centroids were measured for the individual frames and used to derive the offsets used to create the final K and J-band mosaics. In addition to the quasar, observations were made of a nearby ($\Delta r = 11\&5$ arcminutes) star either immediately before (Oct 95 data) or immediately after (Feb

95 data) the observations of the quasar, respectively, in order to obtain an estimate of the point spread function (PSF). During both observing runs the PSF star was imaged in a manner identical to that used for the quasar itself, using the same raster pattern and exposure times (60 seconds per position). From these PSF images the seeing was estimated to be approximately $0.7''$ and $0.5''$ full width at half maximum (FWHM) during the Feb 1995 and Oct 1995 observations of 4C +09.17, respectively. The conditions were photometric during both observing runs, and observations of UKIRT faint standard stars (Casali & Hawarden 1992) provided the flux calibration. Although the seeing was steady during the Oct 95 observing run, it degraded noticeably to $0.9'' - 1.0''$ FWHM during the observations of the standard stars on the Feb 1995 run, making small aperture fluxes derived from the latter data set uncertain. Although both data sets are combined to obtain the deepest possible images of 4C +09.17 (Fig. 1), only the Oct 95 data set is used to derive magnitudes for the individual components and assess the nature of the extended emission in the 4C +09.17 system (Figs. 2 & 3).

Visual images of the 4C +09.17 system were obtained with the Hubble Space Telescope using the Wide Field and Planetary Camera (WFPC2) on 9 September 1994. These images were taken through the F555W filter. The observations of 4C +09.17, along with the results from observations of five other high redshift QSOs with HST, are fully described in Lehnert et al. (1997). The 4C +09.17 data are included here in order to derive the visual-infrared colors of the system.

The Galactic color excess towards 4C +09.17 is $E(B-V) \sim 0.16$ mag (Burstein & Heiles 1982). Using the reddening curves of Savage & Mathis (1979) and Rieke & Lebofsky (1985), we derive a Galactic extinction of $A_V = 0.5$ mag, $A_J = 0.14$ mag and $A_K = 0.06$ mag, respectively. The data presented in the following sections are corrected for these extinctions.

3. Results

The infrared observations reveal a complex structure surrounding the $z=2.1108$, radio loud quasar 4C +09.17. The quasar resides in a system containing three distinct components visible at 2.2 microns, in addition to a resolved, diffuse nebula. The composite K-band mosaic made from the combined Feb 1995 and Oct 1995 data sets is shown in Fig. 1. The brightest companion, $1.72''$ southeast of the quasar and hereafter labelled as component “B”, is clearly resolved, with a structure that appears elongated in the northeast-southwest direction. This object has a K magnitude of 17.87 ± 0.03 mag, and a color of $J-K = 1.56 \pm 0.04$ mag as measured through a $2.0''$ diameter circular beam centered on the emission peak. For comparison, the quasar itself (component “A”) has a K magnitude of 15.76 ± 0.03 mag and a color of $J-K = 1.46 \pm 0.04$ mag. Component “C”, located $2.54''$ northeast of the quasar, has a K magnitude of 19.42 ± 0.07 mag, and a color of $J-K = 2.16 \pm 0.15$ mag. Component C is the reddest member of the 4C +09.17 system. Finally, there is a very faint, diffuse emission region approximately $3''$ southwest of the quasar. This emission has a local maximum, labelled “D” in Fig. 1, approximately $2.9''$ from the quasar, with a K magnitude 20.15 ± 0.13 mag and a J-K color of 1.17 ± 0.17 mag. Component D is found along the direction of the radio jet mapped at 15 GHz by Barthel et al. (1988) and Lonsdale, Barthel, & Miley (1993), but is at a larger distance from the quasar than the radio lobe at a radius of $1.6''$ – marked with a cross in the lower panel of Fig. 1. The magnitudes and colors of the quasar and its companions, corrected for Galactic extinction, are listed in Table 1.

It is clear from Fig. 1 that the entire 4C +09.17 system is surrounded by diffuse infrared emission. In Fig. 2a, we plot the azimuthally averaged K-band surface brightness of the Oct 1995 data out to a radius of $4.5''$. For comparison, the same quantity as a function of radius is plotted for the PSF star taken immediately before the quasar observations. Both profiles have been normalized to the flux within the central three pixels, or $0.45''$. Excess emission above that expected from a point source is clearly seen at all radii. The “bump” in the quasar surface brightness distribution at about $1.5''$ is caused by component B. For comparison, the K-band surface brightness of the quasar and PSF star calculated over a restricted sky position angle of

$262^\circ < \text{PA} < 352^\circ$ (measured east from north) to exclude components B, C and D from the average are plotted in Fig. 2b. The excess over the point spread function is still obvious when the contributions from the quasar companions are removed.

From estimates of the the amount of resolved emission in the J and K-band images, constraints can be placed on the luminosity and color of the emission around 4C +09.17. The FWHM of the PSF images were about $0.5''$ in both the J and K filters during the Oct 95 observations. An estimate of the fraction of the total emission which is resolved around 4C +09.17 has been made by scaling the flux found within a radius of $0.37''$ (2.5 pixels) in the QSO image to that found in the PSF image. Since there is asymmetric structure around 4C +09.17 due to components B, C, and D, we have performed this calculation over the same restricted angle used to generate Fig. 2b. In the K-band, approximately 27% of the total emission beyond a radius of $0.37''$ is resolved, while in the J-band the fraction is about 11%. The total magnitudes of the 4C +09.17 system measured in $8''$ diameter circular beams centered on the QSO (corrected for Galactic extinction) are $K = 15.45$ mag and $J = 16.94$ mag. After removing the contributions of components B, C, and D to the total flux, the resolved emission around 4C +09.17 (beyond a radius of $0.37''$) has $K \sim 17.0$ mag and $J \sim 19.5$ mag. This is slightly brighter than the measurement of Lehnert et al. (1992).

In Figure 3 the infrared and visual flux densities, normalized to the flux density at an observed wavelength of $2.2\mu\text{m}$, are shown for components B, C, and D, as well as the quasar itself. These are overlayed on four representative spectral energy distributions (an observed Im, Scd, Sbc, and an E/S0 galaxy spectrum) taken from Coleman, Wu & Weedman (1980) which have been redshifted to $z = 2.1108$ (Fig. 3a), and $z = 0.84$ (Fig. 3b). The rest-frame UV data have been corrected for Galactic extinction by Coleman, Wu & Weedman.

4. Discussion

The apparent quasar companions are most likely to originate in one of the following ways. First, each could be a foreground galaxy, possibly associated with one or more of the absorption systems seen in the spectrum of 4C +09.17 by Barthel et al. (1990). The three $z_{abs} \ll z_{em}$ (MgII and CIV) absorption line systems in the quasar spectrum provide potential redshifts for the nearby companions. Second, any or all of the companions could be at the same redshift as the quasar, possibly interacting with or accreting onto the quasar host galaxy. If they are at the redshift of 4C +09.17, starlight, ionized gas, and/or scattered AGN light could contribute to the measured infrared fluxes. We deal with each of the infrared components separately below in light of these possibilities.

4.1. Component B

Component B, has recently been shown to be at a redshift of $z = 0.8384$ from an identification of the [OII] 3727Å emission line by Lehnert & Becker (1997). This redshift is consistent with the idea that component B is responsible for the strongest MgII absorption line system in the spectrum of 4C +09.17. At this redshift, the separation on the sky of component B and 4C +09.17 (the MgII “impact parameter”) is about 11.6 kpc. The empirical relationship between impact parameter and rest frame MgII equivalent width found by Lanzetta & Bowen (1990), predicts a separation of 8 – 10 kpc between 4C +09.17 and the absorbing galaxy producing the MgII absorption line, when their data are converted to an $H_0 = 75 \text{ km s}^{-1} \text{ Mpc}^{-1}$. The optical-infrared colors of component B are most similar to those of a late-type spiral galaxy at $z \sim 0.8$ (Fig. 3b). In Fig. 4 the V-J vs. J-K colors of the galaxy templates used in Fig. 3 are plotted as a function of redshift from $z = 0 - 2.2$ in steps of $\Delta z = 0.2$. Also shown in Fig. 4 are three reddening vectors corresponding to the change in J-K and V-J for a rest frame $A_V = 1.0 \text{ mag}$ at $z = 0$, $z = 1.0$ and $z = 2.0$. The galaxies used as templates for the Im, Scd, Sbc and E/S0 Hubble types by Coleman, Wu & Weedman (1980) are shown as observed, i.e. they include intrinsic reddening. Component

B can be reconciled with the Scd curve with a slight amount ($A_V \sim 0.5$ mag) of extra reddening. The J-band magnitude of component B, $J \sim 19.4$ mag, corresponds to a monochromatic luminosity of about $2L^*$ at a rest frame wavelength of 6800\AA . The infrared and visual fluxes are therefore consistent with component B being a late-type spiral galaxy at $z = 0.84$.

4.2. Component C

Due to its proximity (at least in projection), it is natural to ask whether component C could be associated with component B. Component C could be a galaxy at $z \sim 0.8$, yet it is redder than even an old stellar population at this redshift (see Figs. 3b & 4). The J-K and V-J colors of component C imply that the source lies at a fairly large redshift, i.e. $z \geq 1.5$. Although the (3σ) limit on the V magnitude prohibits an accurate estimate of the V-J color of component C, it appears that the colors can be matched by either the Im or the spiral galaxy templates by varying the amount of reddening as long as the galaxy is at a high redshift. If component C is at the redshift of 4C091.7, it may be a $7L^*$ spiral at a projected separation of about 18 kpc. The colors of component C are consistent however, given the V-J limit and the uncertain reddening, with a spiral galaxy at the redshift of the $z = 1.4664$ MgII absorption line system in the spectrum of 4C +09.17. Using the relationship between impact parameter and MgII absorption equivalent width (Lanzetta & Bowen 1990), the 0.46\AA equivalent width would predict a separation of about 40 kpc between component C and the quasar. The measured separation is $2.1''$, or only 17 kpc at $z = 1.466$, implying an expected rest frame equivalent width of $1.0 - 1.5\text{\AA}$. If component C is a spiral galaxy at $z = 1.466$, it has a relatively weak MgII absorption line system (for its measured impact parameter) and a luminosity of about $2L^*$.

4.3. Component D

Component D is fainter and bluer than components B and C. The combination of blue J-K and red V-K colors are quite unlike those expected for a galaxy at the redshift of component B

(see Figs. 3b and 4). It is clear from Fig. 4 that simply reddening any of the galaxy templates will not reproduce the colors of D. Within the uncertainties, the V-J colors of D and B are the same, but D is about 0.3-0.4 mag bluer in J-K. If component D is at the redshift of component B, the H α line is redshifted to $1.208\mu\text{m}$, and lies in the J-band atmospheric window. This line (or more specifically, the H α +[NII] blend) could therefore contribute to the blue J-K color of component D, since there is no correspondingly strong line which is redshifted into the K-band window. To decrease the brightness of component D by 0.3 mag would require an H α +[NII] line flux of about 5.3×10^{-16} erg cm $^{-2}$ s $^{-1}$, corresponding to a luminosity of about 1.4×10^{42} erg s $^{-1}$ at $z = 0.84$. This hypothesized line would have an intrinsic equivalent width of about 420\AA , large even for luminous, high redshift radio galaxies (e.g. Eales & Rawlings 1993). Furthermore, if component D were a spiral galaxy at $z = 0.84$ it would be intrinsically very faint at about $0.3L^*$. The large H α +[NII] luminosity required to account for the blue J-K colors of D coupled with its intrinsically faint overall luminosity make it unlikely that D is a galaxy at $z = 0.84$.

Since D is located along the radio jet/lobe axis of 4C +09.17, and there is known extended Ly α emission line gas at the location of component D which is probably ionized by the quasar, it is unlikely that D is at $z = 0.84$. It is most plausible to suggest that component D is at the redshift of 4C +09.17. If D is at $z = 2.1108$, H α can contribute to the K band flux at $2.04\mu\text{m}$, and [OII] 3727\AA can contribute to the J band flux at $1.16\mu\text{m}$. Heckman et al. (1991) find extended UV continuum and Ly α emission surrounding 4C +09.17. The resolved Ly α flux is $\sim 4 \times 10^{-15}$ erg cm $^{-2}$ s $^{-1}$, corrected for a Galactic extinction of 0.7 mag at 3800\AA (Burstein & Heiles 1982, Savage & Mathis 1979). If the ionized gas around 4C +09.17 has the same Ly α -to-H α emission line flux ratio as found in high redshift radio galaxies, i.e. 3.5 (McCarthy, Elston & Eisenhardt 1992), the expected resolved H α flux is approximately 10^{-15} erg cm $^{-2}$ s $^{-1}$. Heckman et al. note that the resolved Ly α emission in 4C +09.17 is not distributed symmetrically, but is extended more towards the southwest - the direction of both the radio jet and component D. Inspection of their Fig. 1 shows that the radio lobe and component D lie well within the brightest extended Ly α emission line nebula. It is likely therefore, that any emission line contribution to component D comes from gas ionized by the quasar.

As an upper limit to the contribution of emission lines to the K-band flux of component D, we can assign to it all the resolved H α emission line flux estimated from the measured, resolved Ly α emission. When this is done, nearly 73% of the flux from component D could be from H α , and the corrected continuum light has a K ~ 20.8 mag. Performing the same calculation for [OII], and assuming the Ly α -to-[OII] emission line flux ratio is the same in 4C +09.17 as it is in radio galaxies, namely about 8.5 (McCarthy 1993), we estimate that at most 22% of the J-band light seen from component D could be [OII] emission - not as large a fraction as estimated for H α , but still significant.

Subtracting the maximum emission line contributions from the measured J and K-band fluxes makes the continuum J-K color of component D bluer than the redshifted Im galaxy spectral energy distribution in Fig. 3a. If the maximum emission line contribution is used, the continuum from component D is too blue to be starlight at the redshift of 4C +09.17. This conclusion is strengthened if resonant scattering of Ly α photons is an important effect, since then the H α line flux would be larger than we have estimated by using the measured Ly α line flux from Heckman et al. (1991). On the other hand, the H α emission line contribution to the K-band flux of component D may be an upper limit for two reasons. First, the Ly α nebula mapped by Heckman et al. appears larger and more diffuse than component D, so the line emission is probably not concentrated in one area. Second, the H α emission line is near the edge of the K-band atmospheric window at $2.04\mu\text{m}$, and thus the contribution of this line to the integrated K magnitude is dependent upon the kinematics of the emission line gas. However, it nonetheless appears that if component D is at the redshift of 4C +09.17 and emission lines are contributing to the broad band near infrared fluxes, the blue continuum colors are inconsistent with starlight. If component D is at the redshift of 4C +09.17, its continuum flux may be dominated by reflected AGN light and emission lines energized by the quasar.

4.4. The Diffuse Emission around 4C +09.17

In most cases, symmetric, diffuse emission around high redshift quasars is assumed to be at the redshift of the quasar since the likelihood of finding a foreground faint galaxy perfectly centered on the background quasar is very small. The symmetric emission can be starlight, emission line gas, or scattered AGN light. The complex morphology of 4C +09.17 and the coincidence of strong, redshifted emission lines forces us to consider all of these possibilities.

The resolved, diffuse emission beyond a radius of $0.37''$ (Fig. 2b) has a magnitude of $K \sim 17.0$ mag and $J-K \sim 2.5$ mag. This is redder in $J-K$ than any other component in the 4C +09.17 system. The red $J-K$ color of the extended emission seems inconsistent with a strong contribution from scattered AGN light at these wavelengths, unless the scattered light is heavily reddened by dust along the line of sight. If the diffuse emission is starlight, it is extremely luminous, and most similar in color to an evolved stellar population. A K -band magnitude of $K \sim 17.0$ mag implies a $39L^*$ E/S0 host galaxy for 4C +09.17. This luminosity is in fact a lower limit on the true luminosity of the 4C +09.17 host galaxy, since the measurement is made beyond a radius of $0.37''$ from the quasar. At $z = 2.1108$, $0.37''$ is about 3.2 kpc. If the host galaxy follows an $r^{1/4}$ light profile (de Vaucouleurs 1948) with an effective radius of about 4 kpc (Kormendy 1977), the total luminosity of the 4C +09.17 host galaxy could be as much as $70 - 80L^*$. Although extended emission around other high redshift quasars has been taken as evidence for extremely luminous ($> 20L^*$) host galaxies by Lehnert et al. (1992), in the case of 4C +09.17 there are known absorption line systems along the line of sight, implying that some of the light around the quasar must be in the foreground. Component B, which we have associated with the MgII absorption system at $z = 0.84$ is clearly extended. If this galaxy is symmetric, at least in the direction toward and away from 4C +09.17, we estimate that about 10% of its total emission lies at a radius of greater than $2.0''$, i.e. at a large enough distance to contribute to the diffuse emission around the quasar. This flux from component B could be responsible for about 6% of the resolved emission around 4C +09.17. If component B is highly asymmetric toward 4C +09.17, perhaps a result of a galactic arm or tidal tail, the contribution could be larger than 6%, although it seems not to be a

dominant effect.

There is certainly resolved emission line gas around 4C +09.17, as evidenced by the spatially resolved Ly α imaging presented by Heckman et al. (1991). In principle, H α , [NII], and [SII] emission may contribute to the integrated K-band light seen surrounding the quasar. However, even if all the resolved Ly α emission seen by Heckman et al. is used to estimate the resolved H α line flux, less than 5% of the resolved K-band emission around 4C +09.17 could be due to this emission.

5. Summary

Near-infrared images of the radio loud quasar 4C +09.17 show the presence of three “companion” objects with brightnesses of $17.9 < K < 20.2$ mag, as well as resolved, diffuse emission surrounding the quasar. The brightest of these components has been measured to have a $z = 0.8384$ (Lehnert & Becker 1997) and is probably the galaxy responsible for the strong MgII absorption seen in the spectrum of the quasar. The optical-infrared colors of this object are consistent with a late-type spiral galaxy at this redshift, with a luminosity of about $2L^*$. The second brightest companion at K appears most consistent with a star-forming galaxy at $z > 1.5$, and if it is at the redshift of 4C +09.17, it has an intrinsic luminosity of about $7L^*$. If on the other hand, it is a spiral galaxy at a $z \sim 1.5$ it may be associated with the weaker MgII absorption line system at $z = 1.466$, and have a luminosity of about $2L^*$. The faintest member of the 4C +09.17 system has very blue J-K, yet red V-J colors, which appear inconsistent with either an old or young stellar population at the absorption or emission line redshifts associated with 4C +09.17. The unusual colors and diffuse morphology of this component may be explained if it is a combination of strong line emission and scattered QSO light. The fact that it lies along the direction of the radio jet and the extended Ly α emission line gas strengthens this interpretation. The diffuse emission surrounding 4C +09.17 is very bright ($K \sim 17.0$ mag) and redder than the QSO by about one magnitude in J-K. If this emission is starlight at the redshift of 4C +09.17, an elliptical host galaxy with a luminosity larger than about $40L^*$ is implied. Scattered and reddened

AGN light, emission line gas, and flux from absorbing galaxies along the line of sight may all contribute to this emission.

The W.M. Keck Observatory is operated as a scientific partnership between the California Institute of Technology and the University of California. We thank the entire Keck staff, especially Wendy Harrison and Al Conrad, for making these observations possible. In addition, we thank Peter Barthel, Tim Heckman, David Hogg, Neill Reid, Tom Soifer, and Chuck Steidel for helpful discussions. Finally, we would like to thank Steve Warren, the referee, whose comments and suggestions helped to improve the final version of this paper. Infrared astrophysics at Caltech is supported by grants from NASA. This research has made use of the NASA/IPAC Extragalactic Database which is operated by the Jet Propulsion Laboratory, Caltech, under contract with NASA.

REFERENCES

Aaronson, M. A. 1977, Ph D Thesis, Harvard University

Bahcall, J.N., Kirhakos, S., Saxe, D.H. & Schneider, D.P. 1997, ApJ, in press

Barthel, P.D. 1989, Ph.D. Thesis, Leiden University

Barthel, P. D., Miley, G. K., Schlizzi, R. T., & Lonsdale, C. J. 1988, A & A Suppl, 73, 515

Barthel, P. D., Tytler, D.R., & Thomson, B. 1990, A & A Suppl, 82, 339

Boroson, T.A., & Oke J.B. 1984, ApJ, 281, 535

Boroson, T.A., Persson, S.E., & Oke, J.B. 1985, ApJ, 293, 120

Bruzual, G. A. & Charlot, S. 1993, ApJ, 405, 538

Burstein, D., & Heiles, C. 1982, AJ, 87, 1165

Carlberg, R., & Couchman, H. 1989, ApJ, 340, 47

Casali, M.M., & Hawarden, T.G. 1992, UKIRT Newsletter, 3, 33

Coleman, G. D., Wu, C-C. & Weedman, D. W. 1980, ApJS, 43, 393

de Vaucouleurs, G. 1948, Ann. d'Astrophys., 11, 247

Disney, M.J., Boyce, P.J., Blades, J.C., Boksenberg, A., Crane, P., Deharveneng, J.M., Maccheto, F., Mackay, C.D., Sparks, W.B., & Phillipps, S. 1995, Nature, 376, 150

Eales, S.A., & Rawlings, S. 1993, ApJ, 411, 67

Elias, J. H., Frogel, J. A., Matthews, K. & Neugebauer, G. 1982, AJ, 87, 1029

Hartwick, F., & Schade, D. 1990, ARA&A, 28, 437

Heckman, T.M., Lehnert, M.D., van Breugel, W., & Miley, G.K. 1991, ApJ, 370, 78

Hutchings, J.B., Crampton, D., & Campbell, B. 1984, *ApJ*, 280, 41

Hutchings, J.B., & Morris, S.C., 1995, *AJ*, 109, 1541.

Kellerman, K.I., Sramek, R.A., Schmidt, M., Schaffer, D.B., & Green, R.F. 1989, *AJ*, 98, 1195

Kormendy, J. 1977, *ApJ*, 218, 333.

Lanzetta, K., & Bowen, D. 1990, *ApJ*, 357, 321

Lehnert, M.D., Heckman, T.M., Chambers, K.C., & Miley, G.K. 1992, *ApJ*, 393, 68

Lehnert, M.D., & Becker, R., 1997, in preparation.

Lehnert, M.D., van Breugel, W.M., Heckman, T.M., & Miley, G.K. 1997, in preparation.

Lonsdale, C.J., Barthel, P.D., & Miley, G.K. 1993, *ApJ Suppl.*, 87, 63

Malkan, M.A. 1984, *ApJ*, 287, 555

McCarthy, P.J. 1993, *Ann. Rev. Astron. Astrophys.*, 31, 639

McCarthy, P.J., Elston, R., & Eisenhardt, P. 1992, *ApJ*, 387, L29

McLeod, K. K.& Rieke, G. H. 1995, *ApJ*, 454, L77

Mobasher, B., Sharples, R. M.& Ellis, R. S. 1993, *MNRAS*, 263, 560

Neugebauer, G., Matthews, K., & Armus, L. 1995, *ApJ*, 455, L123

Schechter, P. 1976, *ApJ*, 203, 297

Schmidt, M., Schneider, D.P., & Gunn, J.E. 1995, *AJ*, 110, 68

Schneider, D.P., van Gorkom, J.H., Schmidt, M. & Gunn, J.E. 1992, *AJ*, 103, 1451

Smith, E.P., Heckman, T.M., Bothun, G., Romanishin, W., & Balick, B. 1986, *ApJ*, 306, 64

Components in the 4C +09.17 System

Component	Δr	K	J-K	V-K
	''	mag	mag	mag
A=QSO	0.0	15.76 \pm 0.03	1.46 \pm 0.04	3.57 \pm 0.04
B	1.7	17.87 \pm 0.03	1.56 \pm 0.04	4.69 \pm 0.07
C	2.1	19.42 \pm 0.07	2.16 \pm 0.15	> 5.35
D	2.9	20.15 \pm 0.13	1.17 \pm 0.17	4.40 \pm 0.24

Table 1: Near infrared magnitudes and colors of the components in the 4C +09.17 system. All values are measured through circular beams of 2.0'' diameter. Column 1 is the designation used in the text. Column 2, Δr , is the distance of the component from the quasar.

Figure Captions

Fig. 1.— Two views of 4C +09.17 in the K-band. In the top panel, the color palette has been chosen to highlight the quasar (component “A”) and the brightest of the near-infrared companions, component “B”. A solid bar depicting a projected scale of 20 kpc at the redshift of the quasar (for $H_0 = 75 \text{ km s}^{-1} \text{ Mpc}^{-1}$ and $q_0 = 0$) is also shown. In the bottom panel, the color palette has been chosen to highlight the diffuse emission surrounding the system, as well as components “C” (at 1,2) and “D” (at -2,-2). A cross marks the position of the radio lobe mapped by Barthel et al. (1988), and Lonsdale, Barthel & Miley (1993), assuming that the brightest radio component is coincident with the quasar. Component “D” lies along the same direction from the quasar as the radio jet, yet at a larger distance than the radio lobe. In both images, north is up and east is to the left.

Fig. 2.— Azimuthally averaged K-band surface brightness profile of 4C +09.17 in units of relative flux per pixel. In (a) the light is averaged over all angles. In (b) the average is restricted to $262^\circ < \text{PA} < 352^\circ$, chosen to exclude the contribution from components B, C, and D from the average. In both cases the quasar is shown as solid squares and the point spread function (PSF) is shown as open squares. The quasar and the PSF have been normalized to contain the same number of counts within the central $0.45''$.

Fig. 3.— The optical-near infrared flux densities (normalized to the K-band flux density) of the components in the 4C +09.17 system, corrected for a Galactic extinction of $A_V = 0.5$ mag, and overplotted on representative galaxy spectral energy distributions taken from Coleman, Wu & Weedman (1980). The Im galaxy spectrum is a composite of NGC 4449 and NGC 1140, the Scd galaxy spectrum is a composite of M33 and NGC 2403, the Sbc galaxy spectrum is a composite of M51 and NGC 2903, and the E/S0 galaxy spectrum is a composite of the bulges of M31 and M81. All UV spectral points have been corrected for Galactic extinction. The energy distributions have been extended into the near infrared for fig. 3b by matching the J-H and H-K colors of spiral and elliptical galaxies from Aaronson

(1977) to the I-J colors of models with the closest SED match in Bruzual & Charlot (1993). Two redshifts are depicted here, $z = 2.1108$ (Fig 3a), and $z = 0.839$ (Fig 3b), corresponding to the redshift of the quasar as well as the strongest MgII absorption line system seen in the spectrum of 4C +09.17 by Barthel, et al. (1990), respectively. The observed F555W point for component C is an upper limit. The diamond symbol in each plot marks the center of the observed K-band window, to which the individual spectra have been normalized.

Fig. 4.— The V-J vs. J-K colors of components B, C, and D overplotted on the colors expected from the basic galaxy types of Fig. 3 (from Coleman, Wu & Weedman 1980) as a function of redshift between $0 < z < 2.2$, in steps of $\Delta z = 0.2$. The Im galaxy is given by open squares, the Scd galaxy by open triangles, the Sbc galaxy by open circles, and the E/S0 galaxy by solid circles. The data for components B, C, and D are indicated by solid squares and labelled accordingly. The Scd, Sbc, and E/S0 points corresponding to $z = 1$ and $z = 2$ are labelled. In addition, three reddening vectors are shown corresponding to additional extinctions of $A_V = 1$ mag in the rest frame of an object at $z = 0$, $z = 1$, and $z = 2$. The red colors of C indicate a high redshift galaxy, while the colors of D are difficult to fit with any of the generic galaxy types. The optical-infrared colors of component B are consistent with a late type spiral galaxy at a $z \sim 0.84$.

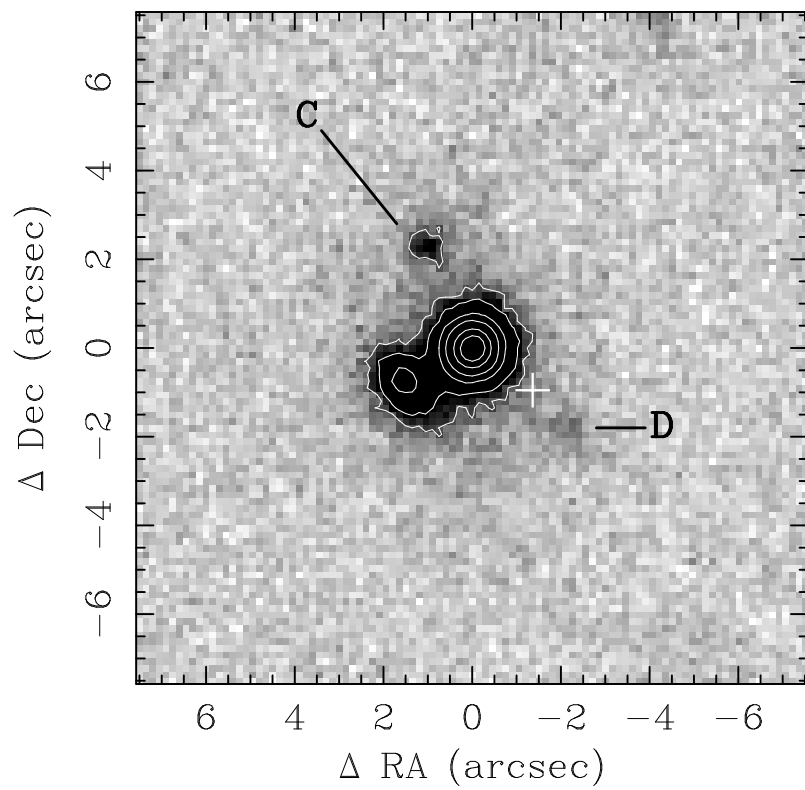
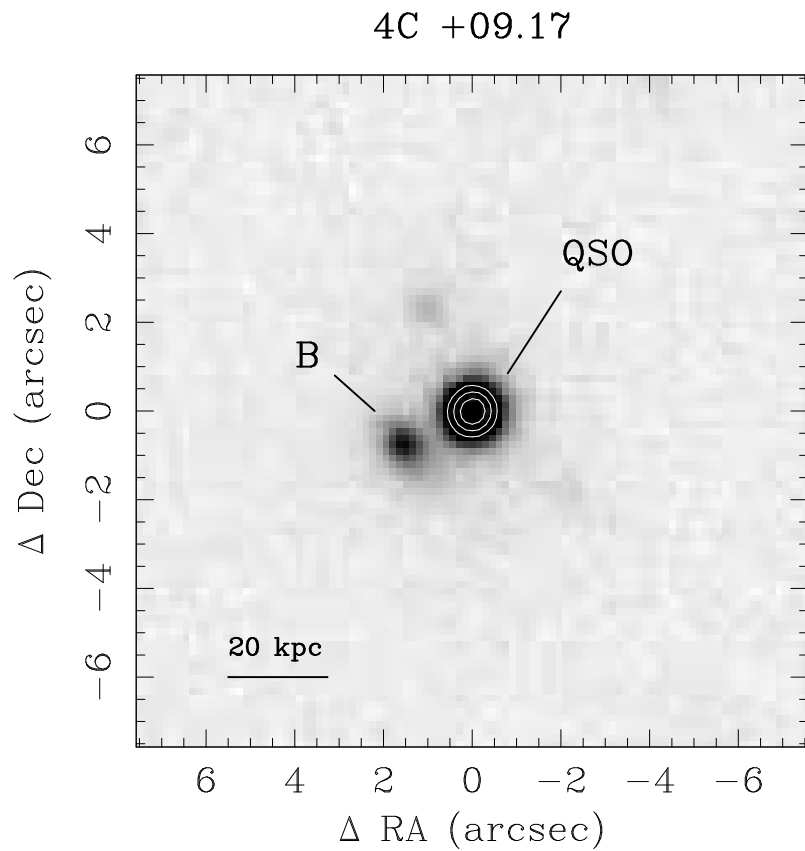


Fig. 1

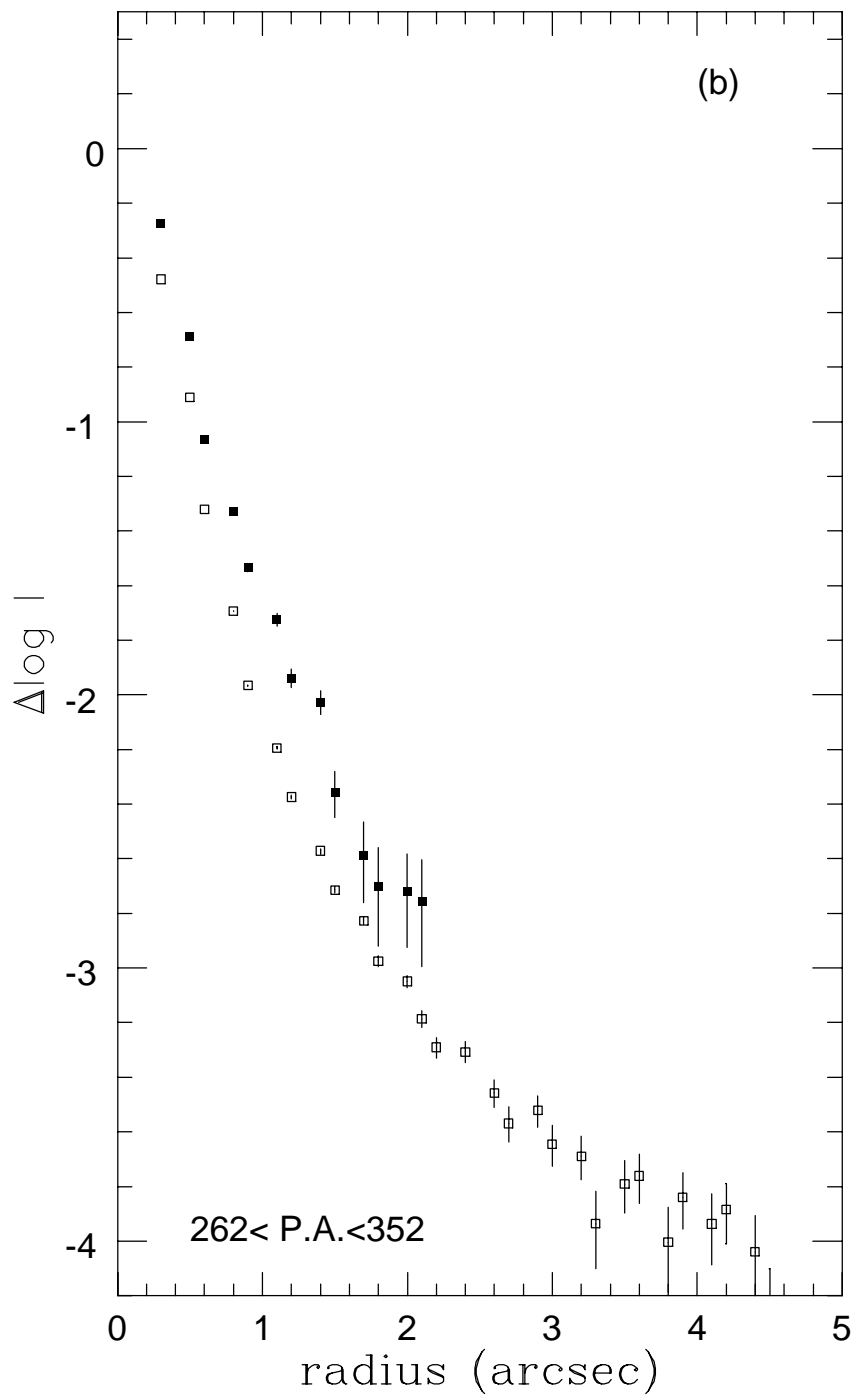
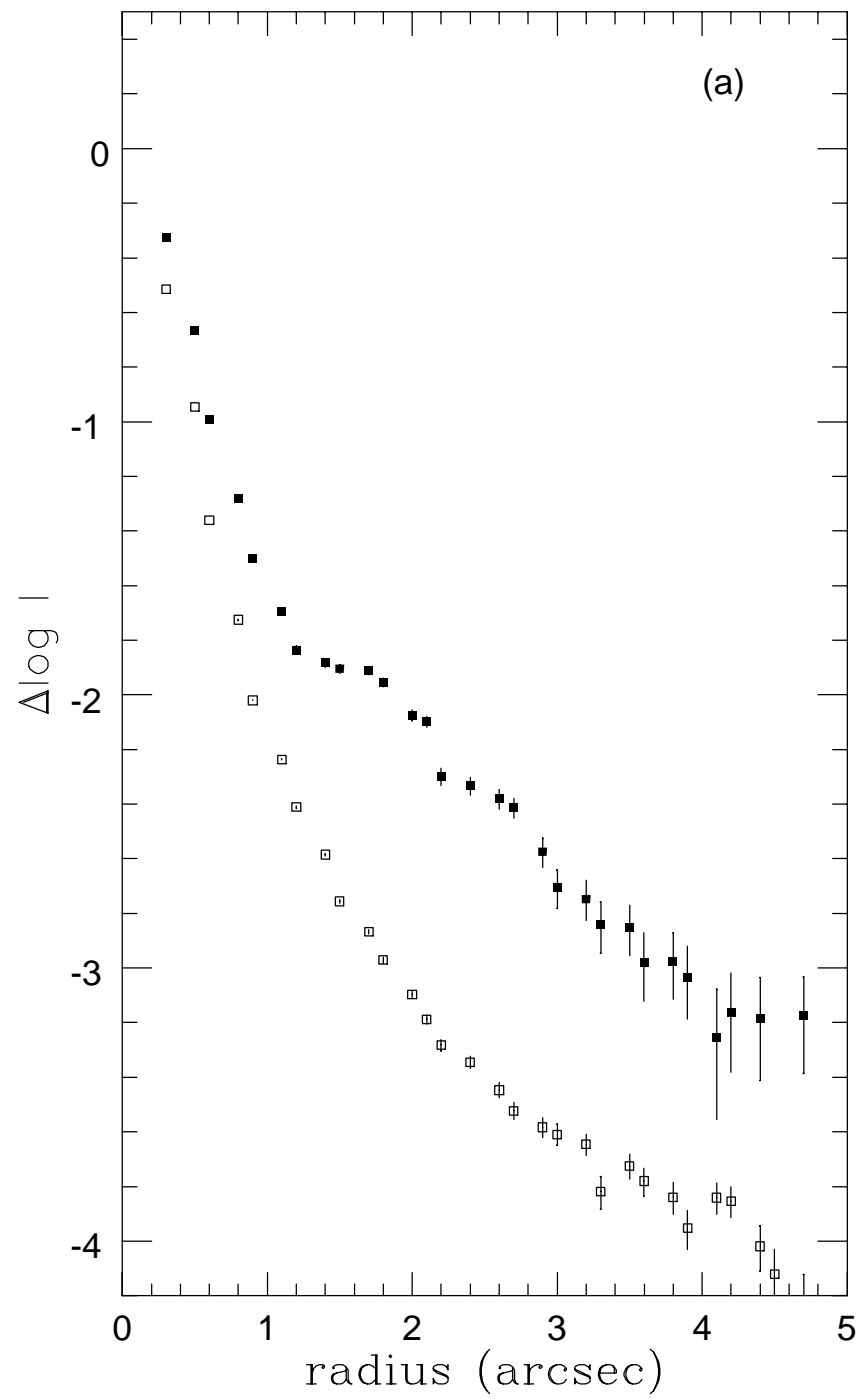


Fig. 2

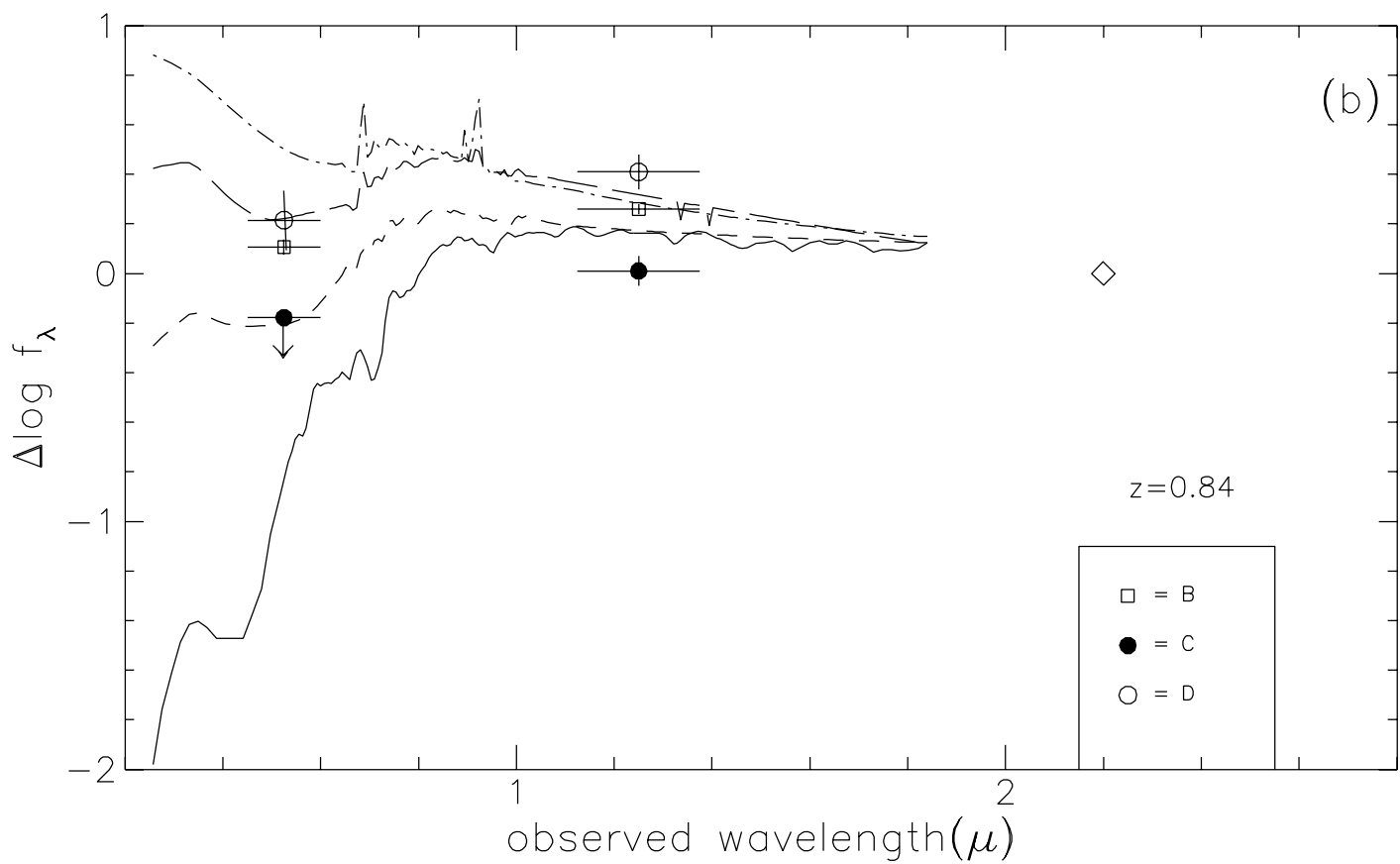
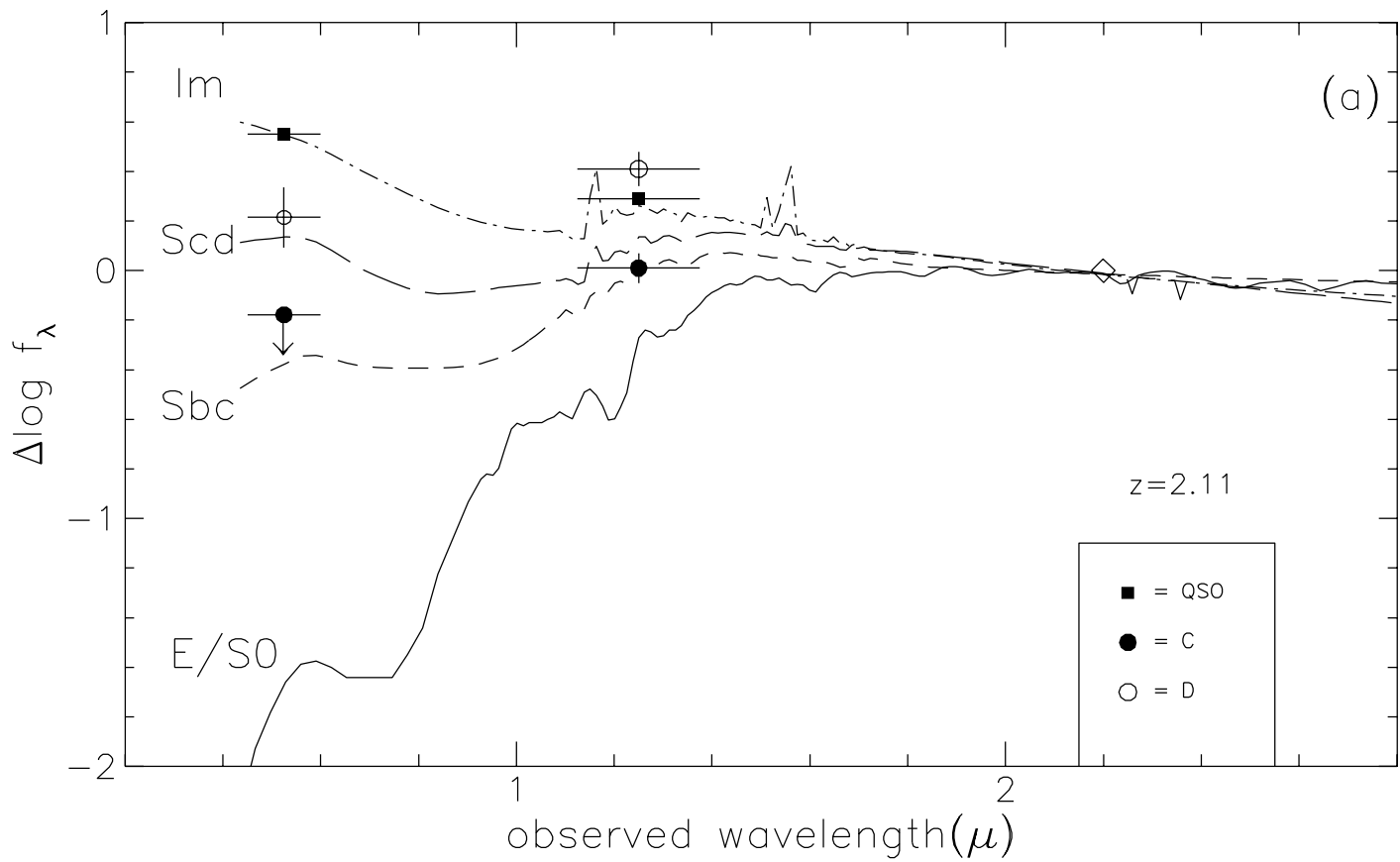


Fig. 3

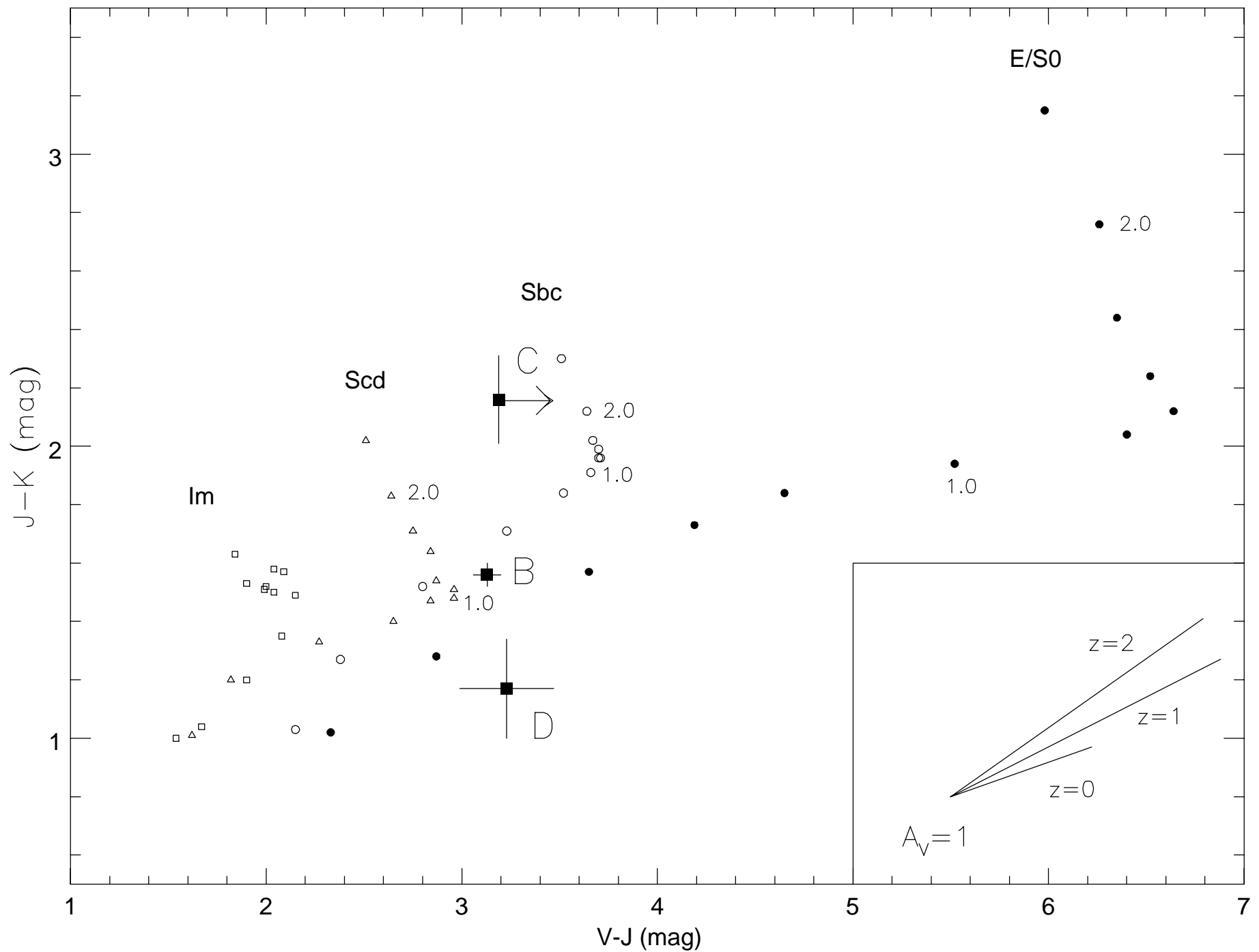


Fig. 4